

HETE-2 LOCALIZATION AND OBSERVATION OF THE BRIGHT, X-RAY-RICH GAMMA-RAY BURST GRB 021211

G. B. CREW,¹ D. Q. LAMB,² G. R. RICKER,¹ J.-L. ATTEIA,³ N. KAWAI,^{4,5} R. VANDERSPEK,¹ J. VILLASENOR,¹ J. DOTY,¹ G. PRIGOZHIN,¹ J. G. JERNIGAN,⁶ C. GRAZIANI,² Y. SHIRASAKI,^{5,7} T. SAKAMOTO,^{4,5,8} M. SUZUKI,⁴ N. BUTLER,¹ K. HURLEY,⁶ T. TAMAGAWA,⁵ A. YOSHIDA,^{5,9} M. MATSUOKA,¹⁰ E. E. FENIMORE,⁸ M. GALASSI,⁸ C. BARRAUD,³ M. BOER,¹¹ J.-P. DEZALAY,¹¹ J.-F. OLIVE,¹¹ A. LEVINE,¹ G. MONNELLY,¹ F. MARTEL,¹ E. MORGAN,¹ T. Q. DONAGHY,² K. TORII,⁵ S. E. WOOSLEY,¹² T. CLINE,¹³ J. BRAGA,¹⁴ R. MANCHANDA,¹⁵ G. PIZZICHINI,¹⁶ K. TAKAGISHI,¹⁷ AND M. YAMAUCHI¹⁷

Received 2003 March 20; accepted 2003 August 22

ABSTRACT

A bright, X-ray-rich gamma-ray burst (GRB) was detected by the French Gamma Telescope (FREGATE) and localized with the Wide Field X-ray Monitor (WXM) and Soft X-ray Camera (SXC) instruments on the *High Energy Transient Explorer 2* satellite (*HETE-2*) at 11:18:34.03 UT (40714.03 SOD) on 2002 December 11. The WXM flight software localized the burst to a $14'$ radius; this was relayed to the astronomical community 22 s after the start of the burst. Ground analysis of WXM and SXC data provided refined localizations; the latter can be described as a circle with a radius of $2'$ centered at R.A. $08^{\text{h}}09^{\text{m}}00^{\text{s}}$, decl. $06^{\circ}44'20''$ (J2000.0). GRB 021211 consists of a single, FRED-like pulse with a duration $t_{90} \approx 2.3$ s at high energies (85–400 keV), which increases to $t_{90} \approx 8.5$ s at low energies (2–10 keV). The peak photon number and photon energy fluxes in the 2–400 keV band are (34.0 ± 1.8) photons $\text{cm}^{-2} \text{s}^{-1}$ and $(1.68 \pm 0.11) \times 10^{-6}$ ergs $\text{cm}^{-2} \text{s}^{-1}$, respectively. The energy fluences in the 2–30 and 30–400 keV energy bands are $S_X = (1.36 \pm 0.05) \times 10^{-6}$ ergs cm^{-2} and $S_\gamma = (2.17 \pm 0.15) \times 10^{-6}$ ergs cm^{-2} , respectively. Thus, GRB 021211 is an X-ray-rich GRB ($S_X/S_\gamma = 0.63 > 0.32$). The average spectrum of the burst is well fitted by a Band function (low-energy power-law index $\alpha = -0.805^{+0.112}_{-0.105}$; high-energy power-law index $\beta = -2.37^{+0.18}_{-0.31}$; and energy of the peak of the spectrum in νF_ν , $E_{\text{peak}}^{\text{obs}} = 46.8^{+5.8}_{-5.1}$ keV). The near-real-time optical follow-up of GRB 021211 made possible by *HETE-2* led to the detection of an optical afterglow for what otherwise would quite likely have been classified as an “optically dark” GRB, since the optical transient faded rapidly (from $R < 14$ to $R \approx 19$) within the first 20 minutes, and was fainter than $R \approx 23$ within 24 hr after the burst. GRB 021211 demonstrates that some fraction of burst afterglows are optically dark because their optical afterglows at times greater than 1 hr after the burst are very faint, and previously have often escaped detection. Such bursts are “optically dim” rather than truly optically dark. GRB 021211 also shows that even such optically dim bursts can have very bright optical afterglows at times less than 20 minutes after the burst.

Subject heading: gamma rays: bursts

On-line material: color figures

1. INTRODUCTION

The bane of the gamma-ray burst (GRB) field is the so-called optically dark burst: that frustrating event for which, despite the best efforts of the satellite observers to provide an accurate and rapid location for the burst, and the diligence of the follow-up community in searching for a

corresponding transient event, in the end, only upper limits on any optical afterglow can be established. In this paper we report on an event that provides a partial answer to the puzzle of such optically dark GRBs.

On 2002 December 11, at 11:18:34.03 UT (40714.03 SOD), the *High Energy Transient Explorer 2* satellite (*HETE-2*; Ricker et al. 2003) detected a GRB (Crew et al.

¹ Center for Space Research, Massachusetts Institute of Technology, 70 Vassar Street, Cambridge, MA 02139.

² Department of Astronomy and Astrophysics, University of Chicago, 5640 South Ellis Avenue, Chicago, IL 60637.

³ Laboratoire d'Astrophysique, Observatoire Midi-Pyrénées, 14 Avenue Est Belin, 31400 Toulouse, France.

⁴ Department of Physics, Tokyo Institute of Technology, 2-12-1 Ookayama, Meguro-ku, Tokyo 152-8551, Japan.

⁵ RIKEN (Institute of Physical and Chemical Research), 2-1 Hirosawa, Wako, Saitama 351-0198, Japan.

⁶ University of California at Berkeley, Space Sciences Laboratory, Berkeley, CA 94720-7450.

⁷ National Astronomical Observatory, Osawa 2-21-1, Mitaka, Tokyo 181-8588, Japan.

⁸ Los Alamos National Laboratory, P.O. Box 1663, Los Alamos, NM 87545.

⁹ Department of Physics, Aoyama Gakuin University, Chitosedai 6-16-1, Setagaya-ku, Tokyo 157-8572, Japan.

¹⁰ Tsukuba Space Center, National Space Development Agency of Japan, Tsukuba, Ibaraki 305-8505, Japan.

¹¹ Centre d'Etude Spatiale des Rayonnements, Observatoire Midi-Pyrénées, 9 Avenue de Colonel Roche, 31028 Toulouse Cedex 4, France.

¹² Department of Astronomy and Astrophysics, University of California, Santa Cruz, 477 Clark Kerr Hall, Santa Cruz, CA 95064.

¹³ NASA Goddard Space Flight Center, Greenbelt, MD 20771.

¹⁴ Instituto Nacional de Pesquisas Espaciais, Avenida dos Astronautas 1758, São José dos Campos 12227-010, Brazil.

¹⁵ Department of Astronomy and Astrophysics, Tata Institute of Fundamental Research, Homi Bhabha Road, Bombay, 400 005, India.

¹⁶ Consiglio Nazionale delle Ricerche, IASF, Sezione di Bologna, via Piero Gobetti 101, 40129 Bologna, Italy.

¹⁷ Faculty of Engineering, Miyazaki University, Gakuen Kibanadai Nishi, Miyazaki 889-2192, Japan.

2002) with the French Gamma Telescope (FREGATE; Atteia et al. 2003). GRB 021211 lasted only a few seconds, but it was bright enough and soft enough to allow the Wide Field X-ray Monitor (WXM; Kawai et al. 2003) to unambiguously locate its position. The Soft X-ray Camera (SXC; Villasenor et al. 2003a) also easily detected the burst. The WXM flight location was relayed to the ground via the burst alert network (Crew et al. 2003; Villasenor et al. 2003b; Vanderspek et al. 2003) 22 s after the start of the burst. *HETE-2* was at this moment emerging from a no-contact zone over the Pacific Ocean—the burst message was caught on the horizon by the *HETE-2* secondary ground station in the Galapagos Islands.

Three robotic telescopes, RAPTOR (Rapid Telescopes for Optical Response), KAIT (Katzman Automatic Imaging Telescope), and Super-LOTIS (Livermore Optical Transient Imaging System), caught the optical transient during the second minute of the event (Wozniak et al. 2002; Li et al. 2002; Park, Williams, & Barthelmy 2002), and a fourth telescope provided the identification of the optical afterglow only 54 minutes after the start of the burst (Fox & Price 2002). However, the afterglow had already faded to $R \approx 19$ at the time of this fourth observation, and subsequent observations showed that it had faded to greater than 23 mag within 24 hr of the burst (Klose et al. 2002; Lamb et al. 2002b; McLeod et al. 2002; Fox et al. 2003b; Pandey et al. 2003). The host galaxy of the burst was identified in *Hubble Space Telescope* (*HST*) images taken on December 18 (Fruchter et al. 2002); soon thereafter, the redshift of the host galaxy was determined to be $z = 1.006$ (Vreeswijk et al. 2002).

The optical afterglow of GRB 021211 is only the third to be caught in near-real-time, the other two being GRB 990123 (Briggs et al. 1999; Akerlof et al. 1999) and GRB 021004 (Shirasaki et al. 2002; Doty et al. 2002; Lamb et al. 2002a; Fox et al. 2003a). The afterglow of GRB 021211 was more than three magnitudes fainter than was the afterglow of GRB 990123 at the same epochs, and about 70% of the searches conducted to date would have failed to detect it one day after the burst (see Berger et al., Fig. 4; Lazzati, Covino, & Ghisellini 2002, Fig. 1; Fox et al. 2003b, Fig. 2).

We turn now to a discussion of the properties of the prompt X-ray and gamma-ray emission from GRB 021211, which will allow a comparison of this event with GRB 990123 (and other bursts with bright optical afterglows), in the hope that such a comparison might shed some light on the nature of optically dark bursts. We show that GRB 021211, while having a duration that is shorter than that of most long-duration bursts and lying near the boundary in duration between long and short GRBs (Hurley 1992; Lamb, Graziani, & Smith 1993; Kouveliotou et al. 1993), is definitely a long burst, by virtue of its spectral properties. Indeed, the burst is X-ray-rich, with a spectrum that peaks at $E_{\text{peak}}^{\text{obs}} \approx 47$ keV. The duration of the burst decreases with increasing energy and exhibits strong spectral evolution from hard to soft, which are also properties that are typical of long GRBs.

2. OBSERVATIONS

2.1. Localization

At the time of the burst, the *HETE-2* spacecraft was pointed $\approx 30^\circ$ away from its nominal antisolar pointing

TABLE 1
GRB 021211 LOCATION HISTORY

Source	$\alpha_{J2000.0}$	$\delta_{J2000.0}$	Radius	Offset
WXM Alert	08 08 57.1	06 42 47	14'	1:1
WXM Update.....	08 08 54.7	06 44 05	14'	1:4
SXC Flight.....	08 09 07.0	06 43 48	...	1:6
WXM Ground.....	08 09 04.8	06 40 41	5'	3:2
SXC Ground.....	08 09 00.0	06 44 20	2'	0:7
Optical Transient.....	08 08 59.858	06 43 37.52	0:1	...

NOTES.—The units of right ascension are hours, minutes, and seconds; those of declination are degrees, arcminutes, and arcseconds. The position error radius is for 90% confidence, and the offset is from the Fox & Price 2002 optical transient.

direction, in order to make calibration observations of the Crab. The burst triggered the FREGATE instrument on the 0.160 s trigger timescale in the FREGATE 85–400 keV energy band. The WXM flight software determined an initial position using the first 3 s of data from the burst; this was relayed to the ground in the “alert” message. Several seconds later it found a better “update” position using the first 4.8 s of data after the trigger: R.A. = $08^{\text{h}}08^{\text{m}}54^{\text{s}}.7$, decl. = $06^\circ 44' 05''$. Both positions were assigned a 14' error radius based on the strength of the image signal to noise ratios (S/N = 29.2 and 33.5 in the X and Y detectors, respectively). The WXM localization was also relayed to the flight SXC software, which correctly localized the burst. However, the SXC flight localization was not sent out to the astronomical community because the calibration of SXC flight localizations had not yet been completed.

Owing to preventive maintenance of the Cayenne Primary Ground Station, burst buffer data were not relayed to the ground until an hour after the burst. The WXM and SXC data were then analyzed (Graziani et al. 2003; Shirasaki et al. 2003; Monnelly et al. 2003), and produced refined localizations that are in good agreement with the WXM flight localization (see Fig. 1). Using a 4–5 s foreground region (similar to the choice made by the flight software), the radius of the 90% confidence region for the burst location is $\approx 3'$ from statistical error alone; including systematic errors, it is conservatively 5'. The SXC analysis was also straightforward. The 2' radius of the final SXC localization, centered at R.A. = $08^{\text{h}}09^{\text{m}}00^{\text{s}}.0$, decl. = $06^\circ 44' 20''$, is dominated by systematic errors. The localization history is summarized in Table 1.

GRB 021211 was observed by other spacecraft in the interplanetary network, and the resulting IPN localization (K. Hurley 2002, private communication) is fully consistent with the WXM and SXC localizations. All of these localizations are consistent with the location of the optical transient (Fox & Price 2002), as shown in Table 1 and Figure 1.

2.2. Temporal Properties

The burst time history is FRED-like (fast rise, exponential decay) and relatively featureless in all energy bands of all instruments. The burst lasts ~ 10 s in the SXC (2–10 keV), as shown in Figure 2a. The SXC data have been binned in 250 ms bins in order to resolve the fast rise of the burst. The duration of the burst in the WXM decreases from ≈ 20 s in the 2–5 keV energy band to ≈ 4 s in the 10–25 keV energy band, as shown in Figures 2b–2d; the data are binned in 100 ms bins. Figures 2e–2h show the time history of the

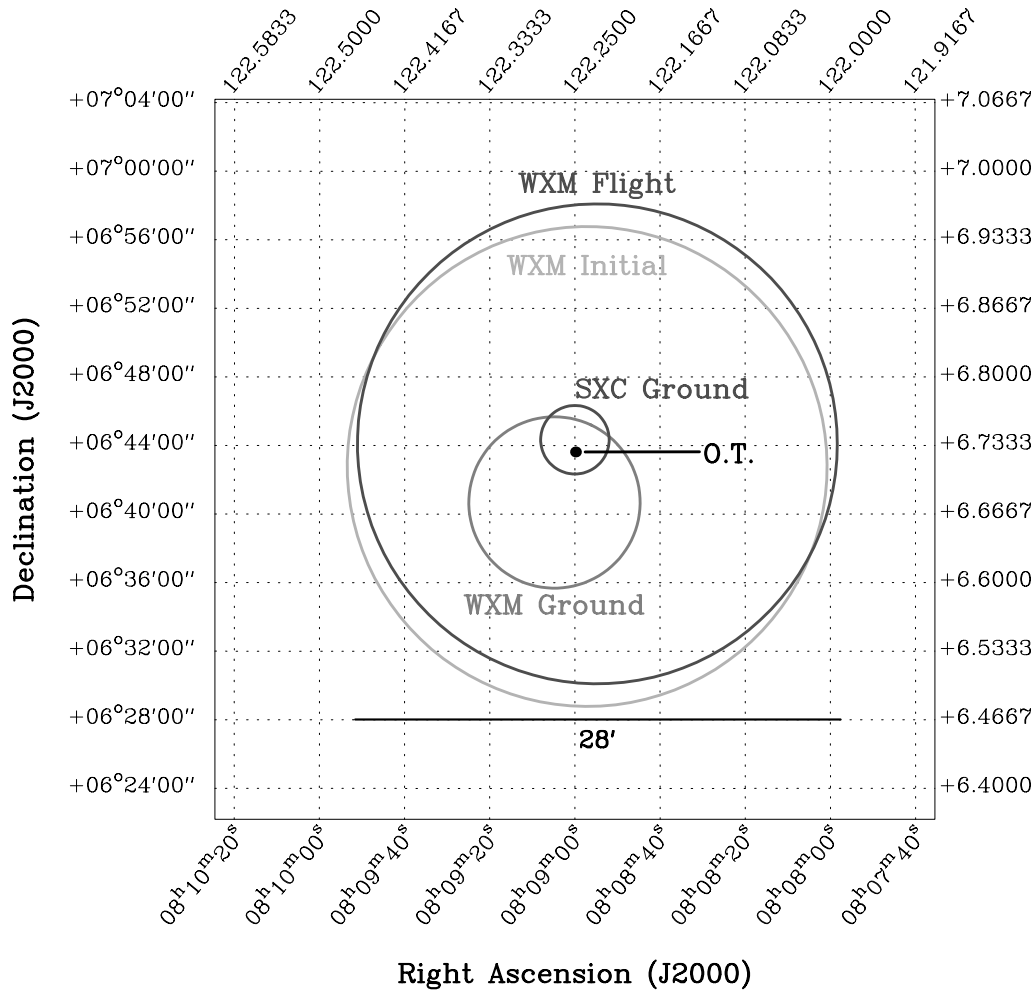


FIG. 1.—Sky map summarizing the localizations reported in the GCN burst position notices (seq. 1–5); cf. Table 1. The 28' diameter for the WXM alert and update flight positions is nominal. [See the electronic edition of the Journal for a color version of this figure.]

burst in various FREGATE energy bands, again binned in 100 ms bins. The duration of the burst decreases to ≈ 2.3 s in the highest FREGATE energy band (85–400 keV).

Table 2 gives the t_{50} and t_{90} durations for various SXC, WXM, and FREGATE energy bands. Figure 3 shows that both duration measures decrease with increasing energy: $t_{50} = 4.2E^{-0.34}$ (where t is in s and E is in keV) and

$t_{90} = 13E^{-0.40}$ (s and keV). This behavior is typical of long-duration GRBs (Fenimore et al. 1995). The SXC and WXM data both suggest a departure from this relation at the lowest energies (< 5 keV), and there is indeed some evidence in the WXM 2–5 keV time history for a weak, soft tail (see Figs. 2b and 3).

2.3. Spectrum

We investigated the average spectral properties of the burst using an interval of 8.0 s, which corresponds to the t_{90} of the burst in the WXM 2–25 keV energy band (see Table 2). To examine the spectral evolution of the burst, we also analyzed the spectra for two subintervals: $t = 0$ –2.3 s, in which the high-energy photons are clearly seen in the FREGATE 85–400 keV band in Figure 2h, and $t = 2.3$ –8.0 s, in which they are absent.

Table 3 presents the results of our time-resolved and time-integrated spectral analysis of the burst. In this analysis, we consider two models: (1) power-law times exponential (PLE; the COMP model in Preece et al. 2000) and (2) Band function (Band et al. 1993). Both the PLE and the Band function models provide satisfactory descriptions of the data: for the PLE model, $\chi^2_{\nu} = 0.78$ (111 degrees of freedom [dof]), while for the Band function, $\chi^2_{\nu} = 0.68$ (110 dof). However, the difference between χ^2_{\min} for the PLE and

TABLE 2
TEMPORAL PROPERTIES OF GRB 021211

Instrument	Energy (keV)	t_{50} (s)	t_{90} (s)
HETE-2 SXC.....	2–10	3.9 ± 0.9	9.6 ± 5.4
	2–25	2.8 ± 0.2	8.0 ± 0.2
	2–10	3.1 ± 0.1	8.5 ± 0.5
	2–5	4.8 ± 0.3	20.2 ± 1.1
	5–10	2.3 ± 0.2	5.4 ± 0.5
HETE-2 WXM.....	10–25	1.9 ± 0.1	3.9 ± 0.2
	6–15	2.01 ± 0.08	4.92 ± 0.50
	15–30	1.53 ± 0.07	4.33 ± 0.33
	30–85	0.93 ± 0.05	2.41 ± 0.15
	85–400	0.86 ± 0.07	2.30 ± 0.52

NOTE.—Errors are 1σ ; the SXC energy range is approximate.

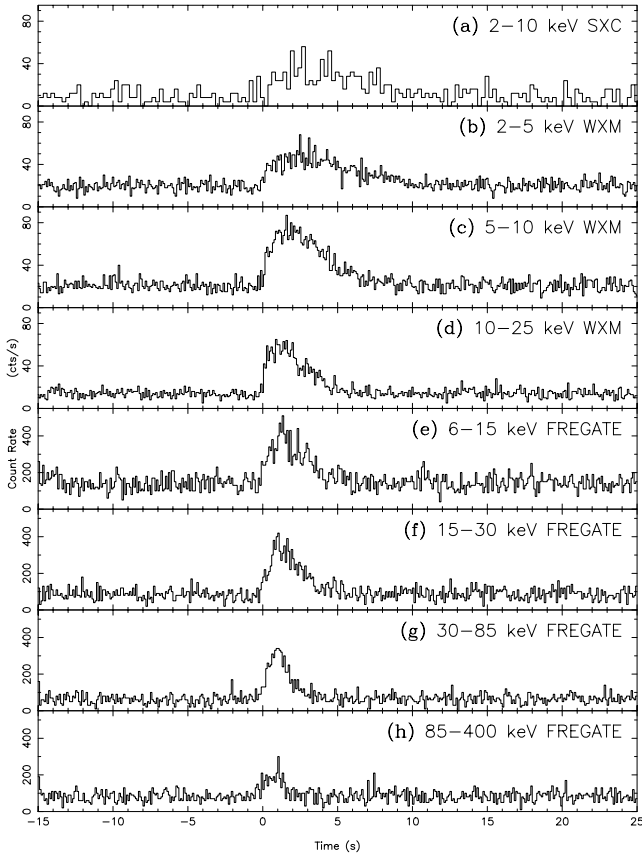


FIG. 2.—Time history of GRB 021211 as observed by the *HETE-2* instruments: (a) all SXC data (2–10 keV) binned in 250 ms bins; WXM data binned in 100 ms bins and (b) 2–5 keV, (c) 5–10 keV, and (d) 10–25 keV bands; and FREGATE data binned in 100 ms bins and (e) 6–15 keV, (f) 15–30 keV, (g) 30–85 keV, and (h) 85–400 keV bands.

Band function models is $\Delta\chi^2 = 11.57$ for one additional parameter. Thus, the Band function is preferred at the 6.7×10^{-4} confidence level.

Figure 4 shows the fit of the Band function to the WXM and FREGATE spectral data. The energy $E_{\text{peak}}^{\text{obs}} = (2 - \alpha)E_0$ of the peak of the νF_ν spectrum is $46.8^{+5.8}_{-5.1}$ keV for the burst-average spectrum, which is at the low end of the range of $E_{\text{peak}}^{\text{obs}}$ values observed by *BATSE* (Preece et al. 2000) and *BeppoSAX* (Amati et al. 2002). Comparing

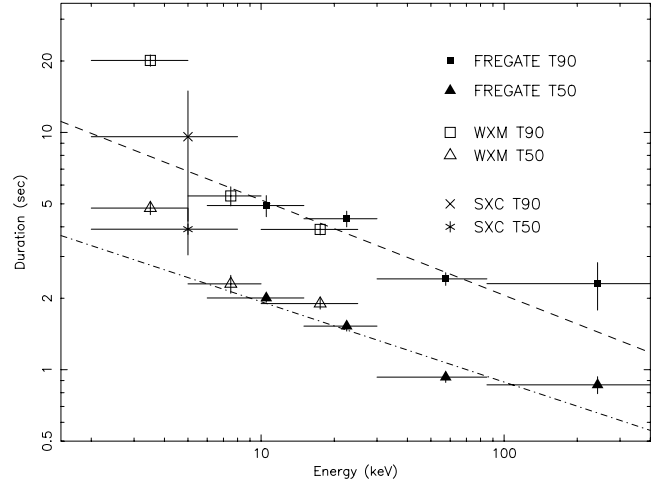


FIG. 3.—Duration of GRB 021211 as a function of energy. The t_{50} and t_{90} values for the FREGATE data increase with decreasing energy as $E^{-0.34}$ and $E^{-0.40}$ (dashed lines), respectively. The FREGATE data were binned into 6–15, 15–30, 30–85, and 85–300 keV bands; the WXM data were binned into 2–5, 5–10, and 10–15 keV bands. The SXC data were not subdivided, and the large error bar is on the t_{90} datum (see Table 2). [See the electronic edition of the *Journal* for a color version of this figure.]

the values obtained when the full interval is split into two subintervals, we find that the spectral index steepens from the first to the second. Likewise, the $E_{\text{peak}}^{\text{obs}}$ value decreases dramatically from $51.6^{+6.2}_{-5.5}$ to $20.6^{+2.7}_{-2.7}$ keV.

The overall emission characteristics of the burst are estimated from the best-fit Band function and summarized in Table 4. In particular, the peak photon number and photon energy fluxes in 1 s are (34.0 ± 1.8) photons $\text{cm}^{-2} \text{s}^{-1}$ and $(1.68 \pm 0.11) \times 10^{-6}$ ergs $\text{cm}^{-2} \text{s}^{-1}$ in the 2–400 keV energy band.¹⁸ The energy fluence over the first 8.0 s of the burst was $S_X = 1.36 \pm 0.05 \times 10^{-6}$ ergs cm^{-2} in the 2–30 keV

¹⁸ We compute the peak photon number flux using the ratio 2.672 of the flux of photons found in the 1 s time interval containing the largest number of photons and the average flux of photons in the 5 s time interval containing the largest number of photons and that brackets the 1 s time interval. We compute the peak photon energy flux in exactly the same way, except that we use the ratio 2.782 of the total photon energy flux (found by weighting each photon with its energy and summing the energies) found in the 1 s time interval containing the largest total photon energy and the average photon energy flux in the 5 s time interval containing the largest total photon energy and that brackets the 1 s time interval.

TABLE 3
SPECTRAL MODEL PARAMETERS FOR GRB 021211

Parameter	$t = 0-2.3$ s	$t = 2.3-8.0$ s	$t = 0-8.0$ s
Cutoff Power Law			
Photon index $\alpha(E^{-\alpha})$	$0.533^{+0.091}_{-0.096}$	$1.071^{+0.165}_{-0.171}$	$0.930^{+0.077}_{-0.079}$
Peak energy (E_{peak})	$66.0^{+3.9}_{-3.6}$	$20.5^{+2.9}_{-2.5}$	$55.9^{+4.3}_{-3.7}$
Cutoff energy (E_0 , keV)	$45.0^{+3.5}_{-4.6}$	$22.1^{+6.2}_{-4.5}$	$52.3^{+7.3}_{-6.1}$
Normalization (at 15 keV)	$0.744^{+0.040}_{-0.038}$	$0.291^{+0.068}_{-0.051}$	$0.345^{+0.020}_{-0.018}$
Band Function			
Index α	$-0.242^{+0.178}_{-0.161}$	$-1.078^{+0.182}_{-0.151}$	$-0.805^{+0.112}_{-0.105}$
Index β	$-2.31^{+0.13}_{-0.23}$	< -2.98	$-2.37^{+0.18}_{-0.31}$
Peak energy ($E_{\text{peak}}^{\text{obs}}$, keV)	$51.6^{+6.2}_{-5.5}$	$20.6^{+2.7}_{-2.7}$	$46.8^{+5.8}_{-5.1}$
Normalization (at 15 keV)	$0.911^{+0.131}_{-0.098}$	$0.287^{+0.074}_{-0.046}$	$0.389^{+0.042}_{-0.034}$

NOTES.—Errors are for 90% confidence. The normalization units are photons $\text{cm}^{-2} \text{s}^{-1} \text{keV}^{-1}$.

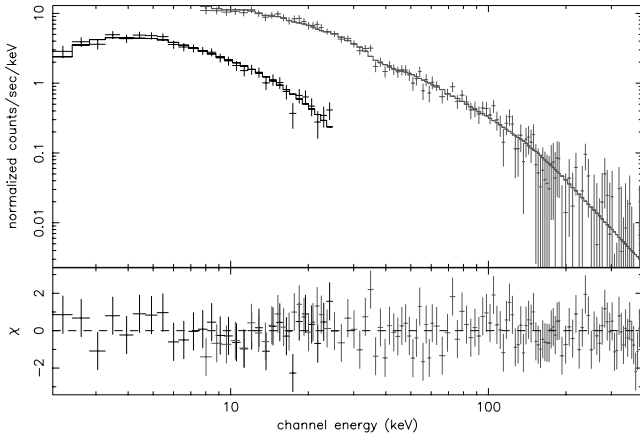


FIG. 4.—Comparison of the observed and predicted spectrum of GRB 021211 in count space, integrated over the first 8.0 s of the burst. The upper panel compares the counts in the WXM energy loss channels (lower energies) and the FREGATE energy loss channels (higher energies) and those predicted by the best-fit Band function spectral model ($\alpha = -0.805^{+0.112}_{-0.105}$, $\beta = -2.37^{+0.18}_{-0.31}$, $E_{\text{peak}}^{\text{obs}} = 46.8^{+5.8}_{-5.1}$ keV); the lower panel shows the residuals to the fit. [See the electronic edition of the *Journal* for a color version of this figure.]

band and $S_{\gamma} = 2.17 \pm 0.15 \times 10^{-6}$ ergs cm^{-2} in the 30–400 keV energy band. This gives a hardness ratio S_X/S_{γ} of 0.63, which is softer than many of the bursts seen by *HETE-2* to date (Barraud et al. 2003) and makes this an X-ray-rich GRB.¹⁹

3. DISCUSSION

3.1. Burst Properties

GRB 021211 was bright, and its duration was relatively short ($t_{50} = 0.86 \pm 0.07$ s and $t_{90} = 2.30 \pm 0.52$ s in the FREGATE 85–400 keV energy band; see Table 2) for a long-duration GRB (Hurley 1992; Lamb et al. 1993; Kouveliotou et al. 1993). The duration of the burst decreases with increasing energy and the spectrum of the burst evolves from hard to soft; both properties are typical of long-duration GRBs. The burst is X-ray-rich, with a soft spectrum having a peak energy of only $E_{\text{peak}} \approx 45$ keV, and

¹⁹ Throughout this paper, we define “X-ray-rich” GRBs and XRFs as those events for which $\log[S_X(2\text{--}30 \text{ keV})/S_{\gamma}(30\text{--}400 \text{ keV})] > -0.5$ and 0.0, respectively.

exhibits a soft tail, which may indicate that the X-ray afterglow of the burst had already begun at this time.

3.2. Optical Follow-up Observations

Previous to GRB 021211, only two GRB optical afterglows had been caught in near-real-time: the optical afterglow of GRB 990123, which was caught by a single robotic telescope (Akerlof et al. 1999), and the optical afterglow of GRB 021004 (another *HETE-2* burst), which was caught by two automated telescopes and a robotic telescope (Fox et al. 2003a).

The real-time localization of GRB 021211 by the WXM flight software, which was rapidly followed by a refined WXM location and an SXC location, both based on ground analysis, led to identification of the optical afterglow in automated, filterless observations, using the 48 inch Schmidt telescope at Mount Palomar, taken 20 minutes after the start of the burst and reported 53 minutes later (Fox & Price 2002).

The prompt reporting of the location of GRB 021211 by the *HETE-2* flight software made possible an unprecedented number of successful near-real-time observations of the optical afterglow by three robotic telescopes: RAPTOR (Wozniak et al. 2002), KAIT (Li et al. 2002), and SuperLOTIS (Park et al. 2002). The observations began 65, 108, and 143 s, respectively, after the start of the burst, and revealed a light curve for the optical afterglow that decreased rapidly during the first 12 minutes ($\propto t^{-1.82 \pm 0.02}$), followed by a slower decline ($\propto t^{-0.82 \pm 0.11}$; Li et al. 2003). The latter decay rate is not atypical of the early-time behavior of GRB afterglows (see Fig. 2 of Fox et al. 2003b).

The host galaxy of the burst was identified in *HST* images taken using the ACS on December 18 UT (six days after the burst) and using the NICMOS on December 24 and 25 UT (12 and 13 days after the burst; Fruchter et al. 2002). Soon thereafter, observations at the European Southern Observatory using the Very Large Telescope showed that the redshift of the host galaxy is $z = 1.006$ (Vreeswijk et al. 2002).

3.3. Implications for the Nature of GRB Jets

GRB 021211 is the second burst for which an exceptionally bright, rapidly decaying component of the optical afterglow has been seen, the other being the famous event GRB 990123 (Briggs et al. 1999; Akerlof et al. 1999). The rapidly decaying component in GRB 990123 has been interpreted as due to emission from the reverse shock resulting from the

TABLE 4
EMISSION PROPERTIES OF GRB 021211

Energy (keV)	Peak Photon Flux (photons $\text{cm}^{-2} \text{s}^{-1}$)	Photon Fluence (photons cm^{-2})	Peak Energy Flux (10^{-7} ergs $\text{cm}^{-2} \text{s}^{-1}$)	Energy Fluence (10^{-7} ergs cm^{-2})
2–10	11.3 ± 1.6	55.6 ± 4.9	1.03 ± 0.12	4.41 ± 0.33
2–25	21.4 ± 1.8	83.4 ± 5.4	3.81 ± 0.19	11.6 ± 0.5
2–30	23.5 ± 1.8	88.1 ± 5.4	4.74 ± 0.21	13.6 ± 0.5
7–30	15.4 ± 0.67	44.6 ± 1.6	4.17 ± 0.17	10.9 ± 0.4
30–400	10.5 ± 0.44	21.7 ± 0.96	12.2 ± 0.89	21.7 ± 1.5
50–100	3.84 ± 0.30	8.32 ± 0.40	4.37 ± 0.33	9.13 ± 0.47
100–300	1.51 ± 0.28	2.64 ± 0.40	4.04 ± 0.63	5.86 ± 1.03
2–400	34.0 ± 1.8	109.8 ± 5.5	16.8 ± 1.1	35.4 ± 1.6

NOTES.—All of the quantities in this table are derived assuming a Band function for the spectrum. Errors are for 90% confidence.

GRB jet striking circumburst material (Sari & Piran 1999a, 1999b). The behavior of the bright, rapidly decaying component of the optical afterglow of GRB 021211 also appears to be consistent with this interpretation (Fox et al. 2003b).

Zhang, Kobayashi, & Mészáros (2003) and Kumar & Panaitescu (2003) have shown that knowledge of both the early-time behavior of the optical afterglow (which is thought to be due to the reverse shock component), and the late-time behavior (which is thought to be due to the forward shock component) provides a diagnostic of whether or not the GRB jet is magnetic energy dominated. A detailed analysis by Kumar & Panaitescu (2003) shows that the early- and late-time behavior of the optical afterglow of GRB 021211 requires that the magnetic energy density in the jet exceed the kinetic energy in the ejecta by a factor ~ 1000 . Zhang et al. (2003) reach a similar conclusion for GRB 990123 (Briggs et al. 1999), the only other GRB that is known to have had an optical afterglow that was very bright at early times (Akerlof et al. 1999).

3.4. Implications for the Nature of Optically Dark GRBs

Two explanations for why some GRBs are not detected optically, despite early and deep follow-up observations, have been widely discussed: (1) the optical afterglow is extinguished by dust in the host galaxy of the burst (see, e.g., Reichart & Price 2002) or (2) the GRB lies at very high redshifts ($z > 5$), and the optical afterglow is absorbed by neutral hydrogen in the host galaxy and in the intergalactic medium along the line of sight from the burst to us (see, e.g., Lamb & Reichart 2000). A third explanation has also been mentioned: some GRBs have optical afterglows that are very faint (Fynbo et al. 2001; Berger et al. 2002; Lazzati et al. 2002).

The optical follow-up observations of GRB 021211 made possible by *HETE-2* show that the optical afterglow of this burst was intrinsically much fainter at late times than most afterglows observed previously. In particular, the optical afterglow of GRB 021211 faded from ≈ 14 mag to fainter than 19 mag within ≈ 20 minutes (Fox & Price 2002) and was fainter than 23 mag within one day (Klose et al. 2002; Lamb et al. 2002b; McLeod et al. 2002; Fox et al. 2003b; Pandey et al. 2003). The afterglow of GRB 021211 was therefore more than 3 mag fainter than the afterglow of GRB 990123 at similar epochs (Akerlof et al. 1999). It was ≈ 2 mag fainter than the faint optical afterglow of GRB 020124 (Berger et al. 2002) at 100 minutes after the burst and remained fainter at all subsequent epochs. It was also fainter at one day than the faint optical afterglows of GRB 980613 (Hjorth et al. 2002) and GRB 000630 (Fynbo et al. 2001).

Indeed, about 70% of the searches conducted to date would have failed to detect GRB 021211 one day after the burst (see Berger et al., Fig. 4; Lazzati et al. 2002, Fig. 1; Fox et al. 2003b, Fig. 2). In addition, according to the statistics compiled by Reichart & Yost (2001, Fig. 1), 65% (15/23) of GRBs for which optical observations had been made with limiting magnitudes $20 < R < 23.5$ 18 hr after the burst were classified as optically dark. It is therefore quite likely that the optical afterglow of GRB 021211 would not have been detected were it not for the real-time localization of the burst by the *HETE-2* WXM and the refined WXM and SXC ground localizations that were rapidly

disseminated, and would therefore have been classified as an optically dark GRB.

Thus, GRB 021211 shows that some fraction of burst afterglows are optically dark because their optical afterglows at times greater than 1 hr after the burst are very faint and previously have often escaped detection. These bursts are “optically dim” rather than truly optically dark. Their existence and properties might lead to an improved understanding of GRBs themselves, as well as burst afterglows. Their existence (as demonstrated by GRB 021211) also suggests that the current sample of burst optical afterglows is not a “fair sample” but is skewed toward bright afterglows.

It is interesting to compare the optical afterglow of GRB 021211 and the optical afterglows of GRB 990123 (Briggs et al. 1999) and GRB 021004 (Shirasaki et al. 2002), the only other bursts for which successful real-time or near-real-time optical afterglow observations have been made (Akerlof et al. 1999; Fox et al. 2003a). The afterglows of both GRB 021211 and GRB 990123 show a rapid decline during the first 20 minutes after the burst, followed by a slower decline, approximately as $\sim t^{-1}$; the latter is similar to the behavior of the afterglows of many GRBs at early times. Indeed, the temporal behaviors of the two afterglows are almost carbon copies of each other, with the exception that the optical afterglow of GRB 021211 is more than 3 mag fainter than that of GRB 990123 at the same epoch (Akerlof et al. 1999; Fox et al. 2003b). In contrast, the optical afterglow of GRB 021004, another burst that was localized in near-real time by *HETE-2* (Shirasaki et al. 2002) and the only other burst for which near-real-time optical afterglow observations have been made (Fox et al. 2003a), exhibited a very different behavior at early times: the afterglow faded only gradually in the first ≈ 2.5 hr after the burst. These results show that the optical afterglows of GRBs exhibit a variety of behaviors at early times and illustrate the fact that *HETE-2* is making it possible to explore the previously unknown behavior of GRB afterglows in the gap in time from the end of the burst to 3–20 hr later that existed during the *BeppoSAX* era.

3.5. Implications for Using GRBs as a Probe of Cosmology

Confirmation that some GRBs have very bright optical afterglows at early times, even if the afterglows are optically dim at late times, has significant implications for using GRB afterglows as a probe of cosmology and the early universe. In particular, the bright early phase of the optical afterglows of GRB 021211 (which lasted ≈ 20 minutes) and GRB 990123 (which lasted ≈ 30 minutes), would have lasted ≈ 1 , 2, and 3.5 hr had these burst occurred at redshifts $z = 5$, 10, and 20, rather than at $z = 1.06$ and $z = 1.6$, respectively. This means that the spectral intensity of the afterglows of GRBs at very high redshifts ($z > 5$) available at a fixed time after the burst for NIR and infrared observations could be much greater within the first few hours than has previously been assumed (Lamb & Reichart 2000; Ciardi & Loeb 2000).

4. CONCLUSIONS

GRB 021211 demonstrates that real-time localization of GRBs is critical to acquiring observations that can help us understand both the transition between the burst itself and its X-ray, optical, and radio afterglows and the distinct,

early behavior of the burst afterglow, including the interpretation that the bright, rapidly fading component is due to emission from a reverse shock.

GRB 021211 also demonstrates that “optically dark” GRBs are due not only to extinction of the optical afterglow by dust in the host galaxy and to absorption of the optical afterglow by neutral hydrogen in the host galaxy and the IGM if there are bursts at very high redshifts, but also because the optical afterglows of some GRBs are much fainter than those observed to date and are therefore not detected. The optical afterglows of these bursts should properly be called “optically dim,” rather than optically dark. However, GRB 021211 shows that even such optically dim bursts can have very bright optical afterglows at times less than 20 minutes after the burst. This suggests that the UVOT on board *Swift* might be able to detect and localize a number of optically dark GRBs. The confirmation that some GRBs have very bright optical afterglows at early times, and that even GRBs whose afterglows are optically dim at late times can have bright afterglows at early times,

also has significant implications for using GRBs and their afterglows as a probe of cosmology and the early universe. It means that the spectral intensity of the afterglows of GRBs at very high redshifts ($z > 5$) at a fixed time after the burst could be much greater within the first few hours than has previously been assumed.

We would like to thank the anonymous referee for comments and suggestions that materially improved the paper. We would also like to thank Scott Barthelmy for sine qua non GCN support. The *HETE-2* mission is supported in the US by NASA contract NASW-4690; in Japan, in part by the Ministry of Education, Culture, Sports, Science, and Technology Grant-in-Aid 13440063; and in France, by CNES contract 793-01-8479. K. H. is grateful for *HETE-2* support under contract MIT-SC-R-293291, for *Ulysses* support under JPL Contract 958056, and for IPN support under NASA grant FDNAG5-11451. G. Pizzichini acknowledges support by the Italian Space Agency.

REFERENCES

- Akerlof, C., et al. 1999, *Nature*, 398, 400
 Amati, L., et al. 2002, *A&A*, 390, 81
 Atteia, J.-L., et al. 2003, in *Gamma-Ray Burst and Afterglow Astronomy 2001*, AIP Conf. Proc. 662, ed. G. R. Ricker & R. K. Vanderspek (New York: AIP), 17
 Band, D., et al. 1993, *ApJ*, 413, 281
 Barraud, C., et al. 2003, *A&A*, 400, 1021
 Berger, E., et al. 2002, *ApJ*, 581, 981
 Briggs, M. S., et al. 1999, *ApJ*, 524, 82
 Ciardi, B., & Loeb, A. 2000, *ApJ*, 540, 687
 Crew, G., et al. 2002, *GCN Circ.* 1734 (<http://gcn.gsfc.nasa.gov/gcn/gcn3/1734.gcn3>)
 ———. 2003, in *Gamma-Ray Burst and Afterglow Astronomy 2001*, AIP Conf. Proc. 662, ed. G. R. Ricker & R. K. Vanderspek (New York: AIP), 66
 Doty, J., et al. 2002, *GCN Circ.* 1568 (<http://gcn.gsfc.nasa.gov/gcn/gcn3/1568.gcn3>)
 Fenimore, E. E., in 't Zand, J. J. M., Noris, J. P., Bonnell, J. T., & Nemiroff, R. J. 1995, *ApJ*, 448, L101
 Fox, D. W., & Price, P. A. 2002, *GCN Circ.* 1731 (<http://gcn.gsfc.nasa.gov/gcn/gcn3/1731.gcn3>)
 Fox, D. W., et al. 2003a, *Nature*, 422, 284
 ———. 2003b, *ApJ*, 586, L5
 Fruchter, A. S., et al. 2002, *GCN Circ.* 1781 (<http://gcn.gsfc.nasa.gov/gcn/gcn3/1781.gcn3>)
 Fynbo, J. U., et al. 2001, *A&A*, 369, 373
 Graziani, C., et al. 2003, in *AIP Conf. Proc. 662, Gamma-Ray Burst and Afterglow Astronomy 2001*, ed. G. R. Ricker & R. K. Vanderspek (New York: AIP), 114
 Hjorth, J., et al. 2002, *ApJ*, 576, 113
 Hurley, K. 1992, in *AIP Conf. Proc. 265, Gamma-Ray Bursts*, ed. W. Paciesas & G. Fishman (New York: AIP), 3
 Kawai, N., et al. 2003, in *AIP Conf. Proc. 662, Gamma-Ray Burst and Afterglow Astronomy 2001*, ed. G. R. Ricker & R. K. Vanderspek (New York: AIP), 25
 Klose, S., et al. 2002, *GCN Circ.* 1739 (<http://gcn.gsfc.nasa.gov/gcn/gcn3/1739.gcn3>)
 Kouveliotou, C., et al. 1993, *ApJ*, 413, L101
 Kumar, P., & Panaitescu, A. 2003, *ApJ*, submitted (astro-ph/0305446)
 Lamb, D. Q., Graziani, C., & Smith, I. A. 1993, *ApJ*, 413, L11
 Lamb, D. Q., & Reichart, D. E. 2000, *ApJ*, 536, 1
 Lamb, D. Q., et al. 2002a, *GCN Circ.* 1600 (<http://gcn.gsfc.nasa.gov/gcn/gcn3/1600.gcn3>)
- Lamb, D. Q., et al. 2002b, *GCN Circ.* 1744 (<http://gcn.gsfc.nasa.gov/gcn/gcn3/1744.gcn3>)
 Lazzati, D., Covino, S., & Ghisellini, G. 2002, *MNRAS*, 330, 583
 Li, W., Filippenko, A. V., Chornock, R., & Jha, S. 2003, *ApJ*, 586, L9
 Li, W., et al. 2002, *GCN Circ.* 1737 (<http://gcn.gsfc.nasa.gov/gcn/gcn3/1737.gcn3>)
 McLeod, B., et al. 2002, *GCN Circ.* 1750 (<http://gcn.gsfc.nasa.gov/gcn/gcn3/1750.gcn3>)
 Monnelly, G., et al. 2003, in *AIP Conf. Proc. 662, Gamma-Ray Burst and Afterglow Astronomy 2001*, ed. G. R. Ricker & R. K. Vanderspek (New York: AIP), 49
 Pandey, S. B., et al. 2003, *A&A*, 408, L21
 Park, H. S., Williams, G., & Barthelmy, S. 2002, *GCN Circ.* 1736 (<http://gcn.gsfc.nasa.gov/gcn/gcn3/1736.gcn3>)
 Preece, R. D., et al. 2000, *ApJS*, 126, 19
 Reichart, D. E., & Price, P. A. 2002, *ApJ*, 565, 174
 Reichart, D. E., & Yost, S. A. 2001, preprint (astro-ph/0107545)
 Ricker, G. R., et al. 2003, in *AIP Conf. Proc. 662, Gamma-Ray Burst and Afterglow Astronomy 2001*, ed. G. R. Ricker & R. K. Vanderspek (New York: AIP), 3
 Sari, R., & Piran, T. 1999a, *ApJ*, 517, L109
 ———. 1999b, *ApJ*, 520, 641
 Shirasaki, Y., et al. 2002, *GCN Circ.* 1565 (<http://gcn.gsfc.nasa.gov/gcn/gcn3/1565.gcn3>)
 ———. 2003, in *AIP Conf. Proc. 662, Gamma-Ray Burst and Afterglow Astronomy 2001*, ed. G. R. Ricker & R. K. Vanderspek (New York: AIP), 117
 Vanderspek, R. K., et al. 2003, in *AIP Conf. Proc. 662, Gamma-Ray Burst and Afterglow Astronomy 2001*, ed. G. R. Ricker & R. K. Vanderspek (New York: AIP), 101
 Villaseñor, J. N., et al. 2003a, in *AIP Conf. Proc. 662, Gamma-Ray Burst and Afterglow Astronomy 2001*, ed. G. R. Ricker & R. K. Vanderspek (New York: AIP), 33
 ———. 2003b, in *AIP Conf. Proc. 662, Gamma-Ray Burst and Afterglow Astronomy 2001*, ed. G. R. Ricker & R. K. Vanderspek (New York: AIP), 107
 Vreeswijk, P., et al. 2002, *GCN Circ.* 1785 (<http://gcn.gsfc.nasa.gov/gcn/gcn3/1785.gcn3>)
 Wozniak, P., et al. 2002, *GCN Circ.* 1757 (<http://gcn.gsfc.nasa.gov/gcn/gcn3/1757.gcn3>)
 Zhang, B., Kobayashi, S., & Mészáros, P. 2003, *ApJ*, 595, 950